Journal of Applied Polymer Science

Removal of Copper(II) Ions with a Thermoresponsive Cellulose-*g*-Poly(*N*-isopropyl acrylamide) Copolymer

Hasine Kasgoz, Zehra Ozbas, Emine Esen, Canan Puren Sahin, Gulten Gurdag

Department of Chemical Engineering, Faculty of Engineering, University of Istanbul, Avcilar Campus 34320, Avcilar-Istanbul, Turkey

Correspondence to: H. Kasgoz (E-mail: hasineka@istanbul.edu.tr)

ABSTRACT: *N*-Isopropyl acrylamide monomer was grafted onto cellulose (Cell) with a cerium(IV) ammonium nitrate (CAN)–nitric acid initiator system, and a thermoresponsive Cell-*g*-poly(*N*-isopropyl acrylamide) (PNIPAM) copolymer was obtained. The copolymer was characterized with Fourier transform infrared spectroscopy, X-ray diffraction, and scanning electron microscopy/electron-dispersive spectrometry analysis. The lower critical solution temperature (LCST) of the copolymer was determined by differential scanning calorimetry technique. The swelling capacities and water retention values were determined in distilled water in the temperature range from 10 to 50°C. The adsorption experiments were performed by a solid-phase extraction technique. Sodium dodecyl benzene sulfonate (SDBS) was used as an extractant, and Cu(II) ion was complexed with SDBS before the adsorption process. Then, the adsorption of the Cu(II)–SDBS complexes onto Cell-*g*-PNIPAM copolymers through hydrophobic interaction was performed at higher temperatures than the LCST of the copolymer. The adsorption capacity (Q) was dependent on the initial pH of the metal-ion solution, and Q decreased at lower pHs. The maximum sorption capacity of the copolymer for the Cu(II) ion was 1.18 mmol/g, and a high amount of sorption equilibrium was attained in 10 h. We found that the adsorption kinetics followed a pseudo-second-order kinetic model. The adsorption experiments showed that the adsorption was S-type according to the Giles classification system. It was also determined that the thermoresponsive Cell copolymer could be used for the removal of Cu(II) ions as an environmentally friendly sorbent. © 2013 Wiley Periodicals, Inc. J. Appl. Polym. Sci. 130: 4440–4448, 2013

KEYWORDS: adsorption; functionalization of polymers; stimuli-sensitive polymers

Received 5 December 2012; accepted 10 May 2013; Published online 24 July 2013

DOI: 10.1002/app.39527

INTRODUCTION

Water pollution with heavy-metal ions is a serious problem because of the toxicity of metal ions to human beings and other living organisms.[1,2] Their effective removal from industrial wastewater has great importance from both scientific and practical perspectives. For this purpose, various methods, including chemical precipitation, membrane separation, solvent extraction, ion exchange, and adsorption, have been developed.[3–5] Among these methods, adsorption is a very promising technique because of its high efficiency, easy handling, and availability of various adsorbents.[5–7] In previous studies in the literature, a large number of polymeric materials have been used as adsorbents for the removal of heavy-metal ions.[8–12] Thermosensitive polymers, which can performed a temperature swing adsorption, have also been used as adsorbents.[13–19] The temperature swing adsorption technique has attracted attention because of both the simplicity of the process and the reduction in the amount of waste and its environmentally friendly characteristics. In the process, adsorption and desorption occurs only by changes in the temperature. Most thermosensitive polymers are based on poly(*N*-isopropyl acrylamide) (PNIPAM), which exhibits hydrophilicity and hydrophobicity in water at temperatures lower and higher than the lower critical solution temperature (LCST), respectively.

Thermosensitive polymeric adsorbents[14,15,18] composed of PNIPAM (the primary component) and a chelating or an ionic component (the secondary component) were used in the removal of heavy-metal ions from aqueous solutions. However, the amount of secondary components having functional groups capable of complexing with metal ions is limited to less than a few molar percentage of *N*-isopropyl acrylamide (NIPAM) because an increase in the secondary component results in a lack of thermosensitivity. This limitation leads to a low adsorption capacity (Q). On the other hand, the use of PNIPAM gel in the adsorption process in the presence of an extractant has been examined in some studies.[13,16,17] However, the diffusion of big metal-extractant molecules into the gel structure has a limited Q. Another choice in the adsorption process is the use of a

water-soluble thermosensitive polymer, but in that case, the desorption process must be performed in a membrane. On the basis of the previous studies, the use of a linear thermosensitive polymer attached to a solid substrate in the presence of an extractant would be more effective for the removal of metal ions from aqueous solutions. In addition, the usability of different extractants in the process would be an advantage for the selective adsorption of metal ions from aqueous solutions.

Cellulose (Cell) is the most abundant renewable organic material.[20] Various techniques are available for modification of Cell, and graft polymerization with a suitable monomer is an indispensable technique for Cell modification without any loss in its original properties.

In this study, by considering the literature studies, we aimed to use thermosensitive Cell fibers as adsorbents for the removal of metal ions from aqueous solutions for the first time. For this purpose, NIPAM polymer was grafted onto Cell fiber, and a thermosensitive Cell copolymer with a high graft ratio was obtained. The copolymer was characterized by Fourier transform infrared (FTIR) spectroscopy, X-ray diffraction (XRD), scanning electron microscopy (SEM), and differential scanning calorimetry (DSC) analysis. The application of the graft product as an adsorbent for the removal of Cu(II) ions was evaluated, and the effects of various adsorption parameters on the removal capacity were investigated.

EXPERIMENTAL

Materials

α-Cell powder was obtained from Sigma-Aldrich. NIPAM was purchased from Acros. Cerium(IV) ammonium nitrate (CAN), sodium dodecyl benzene sulfonate (SDBS), nitric acid, potassium bromide, sodium hydroxide, and hydrochloric acid were Merck products. Ammonium persulfate and *N,N,N′,N′*-tetramethylethylenediamine were purchased from Riedel-de Haen and Serva Electrophoresis GmbH, respectively.

Preparation of the Cell-*g*-PNIPAM Copolymer

The graft copolymerization of NIPAM onto Cell was carried out in a three-necked, round-bottomed flask fitted with a mechanical stirrer at 30.0 ± 0.1°C for 10 h. In the preliminary experiments, the optimum parameters, including the monomer and initiator concentration, initiator/acid ratio, and reaction time, were examined. The reaction parameters by which the product had the highest graft value and swelling capacity were obtained and were chosen as the optimum reaction parameters.[21] Before grafting, 3 g of Cell and 12.7 g of NIPAM monomer were added to the three-necked, round-bottomed flask containing 150 mL of a solution of nitric acid ($2.5 \times 10^{-3}M$), and the mixture was purged with nitrogen gas for about 30 min to remove oxygen. To initiate the grafting, CAN was added to the reaction mixture, and the reaction was carried out for 10 h. The initiator was divided into four equal portions, and each portion was added at equal time intervals. The total concentration of CAN was $12 \times 10^{-3}M$. After the reaction, the mixture was washed with a large amount of distilled water to remove the unreacted monomer, linear homopolymer, and impurities. Finally, the graft copolymer was dried *in vacuo* at 40°C to give a fine white powder.

In the FTIR, XRD, and SEM characterization studies, linear PNIPAM was prepared by the polymerization of NIPAM monomer (0.75*M*, 10 mL) in the presence of ammonium persulfate (6.85 mg) and *N,N,N′,N′*-tetramethylethylenediamine (9 μL) at room temperature for 24 h for comparison purposes.

Characterization Studies

FTIR spectra of the dry powder samples were recorded with a PerkinElmer Precisely Spectrum One model instrument in the range from 4000 to 400 cm^{-1} with KBr pellets (1:200). XRD analyses of samples were performed with a Rigaku D/Max-2200/PC model wide-angle XRD instrument (Rigaku, Japan) with a Cu anode and running at 40 kV and 40 mA with scanning from 2 to 15° at 0.05°/min. SEM photographs of the products were taken by an FEI Quanta 450 FEG model scanning electron microscope operating at an accelerating voltage of 2–10 kV and equipped with an electron-dispersive spectrometry (EDS) instrument. The samples were coated with a thin layer of gold with a coating unit before testing. Elemental analysis was performed with a Thermo Finnigan Flash EA 1112 model instrument. The LCST values of the products were determined by a Seiko II Exstar 6000 DSC instrument with heating from 10 to 70°C at a heating rate of 1°C/min with distilled water as a reference.

Determination of the Graft Yield (%*G*) and Efficiency of Grafting (G_E). %*G* and G_E were calculated according to the nitrogen content (%) obtained from the elemental analysis results:

$$\text{Graft Yield}\,(\%\text{G}) = (\text{N}/\text{N}_0) \times 100 \quad (1)$$

where *N* and N_0 are the nitrogen content of the graft copolymer and NIPAM monomer, respectively.

$$\text{Efficiency of Grafting}\,(\%\text{G}_E) = (\text{Amount of NIPAM grafted}/\text{Total amount of NIPAM in the feed}) \times 100 \quad (2)$$

Determination of the Swelling Degree (*S*%). *S*% of the graft copolymer was determined gravimetrically by the tea-bag method in the temperature range from 10 to 50°C. A tea bag containing 0.5 g of sample was immersed in distilled water at the indicated temperature. It was taken out of the water, wiped superficially with a filter paper, and weighed at certain time intervals. *S*% was calculated from the following equation:

$$\text{S}\,\% = (\text{W}_\text{s} - \text{W}_\text{d})/\text{W}_\text{d} \times 100 \quad (3)$$

where W_s and W_d are the weights of the swollen and dry samples, respectively.

Adsorption Studies

The dry polymer (0.5 g) and SDBS aqueous solution (100 mmol/L, 20 mL) were mixed in a vial. Then, a Cu^{2+} solution (50 mmol/L, 20 mL) was added to the polymer–surfactant mixture, and the vial was shaken in a water bath at 10°C for 24 h to allow the polymer to swell. After swelling, the vial was heated to 50°C and kept at this temperature for 48 h to attain equilibrium. During this process, the concentration of Cu^{2+} ions at

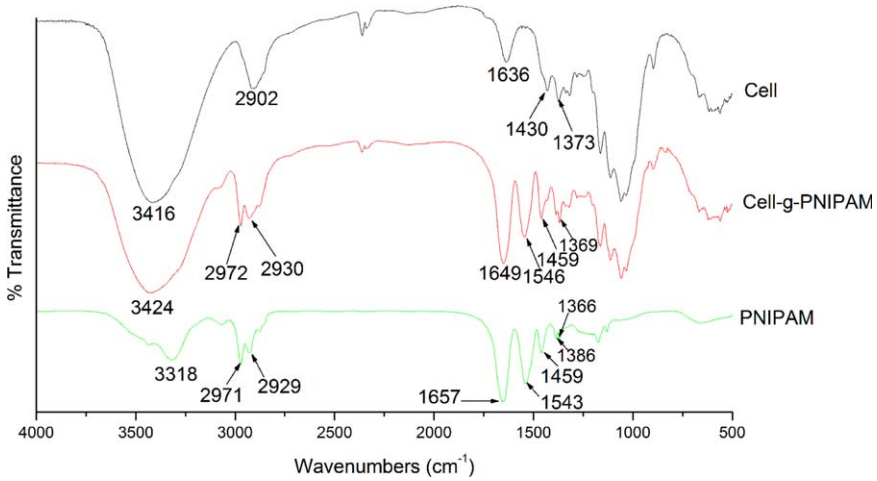

Figure 1. FTIR spectra of Cell, PNIPAM, and their graft copolymer (Cell-*g*-PNIPAM). [Color figure can be viewed in the online issue, which is available at wileyonlinelibrary.com.]

certain time intervals was determined with an atomic absorption spectrometer. The determination of the metal-ion concentration was done with a PerkinElmer 2000 series atomic absorption spectrometer. The Q (mmol/g) values of the graft copolymer were calculated with the following equation:

$$Q\,(\text{mmol/g}) = (C_i - C_e)V/m \tag{4}$$

where C_i and C_e are the concentration of Cu(II) ions in the initial solution and after adsorption for different periods of time (mmol/g), respectively; V is the volume of the solution added (L); and m is the amount of polymer (g).

Q of the graft copolymer was also determined in the pH range 3.0–6.0. The pH of the initial solution was adjusted with dilute HCl or NaOH. The residual concentrations of Cu(II) ions were determined as described previously. Also, the adsorption and desorption cycles were performed at 50 and 10°C, respectively. The concentration of Cu(II) ions for each cycle was determined, and the capacity was calculated as described previously.

RESULTS AND DISCUSSION

FTIR Characterization

The FTIR spectra of Cell, PNIPAM, and graft copolymer (Cell-*g*-PNIPAM) are given in Figure 1. In the spectrum of Cell, the absorption bands at 3400 and 2900 cm^{-1} were attributed to the stretching of O—H and C—H bonds. The bands at 1636 and 1430 cm^{-1} were due to the bending vibrations of absorbed water and the in-plane bending vibrations of H—CH and O—CH groups, respectively.[22,23] In the spectrum of PNIPAM, the bands at 1657 and 1543 cm^{-1} were due to the stretching vibrations of C=O (amide I band) and N—H/C—N bonds (amide II band), respectively.[23–25] Absorption bands originating from isopropyl groups [—$CH(CH_3)_2$] at 1366 and 1386 cm^{-1} were also observed.[24] The presence of all of the characteristic peaks of Cell and PNIPAM in the spectrum of the graft copolymer confirmed the grafting of NIPAM onto Cell. The appearance of an absorption band originating from N—H/C—H bonds at 1547 cm^{-1} was more proof for the grafting reaction.

XRD Analysis

From the XRD studies (Figure 2), we observed that Cell on a 2θ scale showed peaks at 17.5° (the distance between layers, $d = 5.06$ Å) and 22.5° ($d = 3.95$ Å) and that PNIPAM showed peaks at 8.6° ($d = 10.17$ Å) and 19.9° ($d = 4.46$ Å) due to the crystalline regions in the polymer matrix. In XRD pattern of Cell-*g*-PNIPAM, the peaks originating from both Cell and PNIPAM were observed together.

SEM Observation

SEM images of the PNIPAM, Cell, and graft copolymer are given in Figures 3 and 4. As shown in Figure 3(a), PNIPAM had a smooth and strict structure. Cell fibers [Figure 3(b)] also exhibited a relatively smooth surface compared with the graft copolymer (Figure 4). The changing of the Cell fibers after copolymerization was observed clearly in the SEM images with different magnitudes of the graft copolymer (Figure 4). In Figure 4, the graft chains of PNIPAM grown and deposited on the surface of the Cell fibers and the thickening of the fibers are clearly visible.

%*G*

%*G* was calculated according to the nitrogen content of the product. The nitrogen content was determined as 8.60%, and %*G*, which was the PNIPAM content per 100 g of total product, was calculated as 69.5%. In addition, G_E was found to be 85.9%. There are various studies in the literature on the grafting of NIPAM monomer onto Cell fiber, and these studies used various grafting methods, including photopolymerization and atom transfer radical polymerization.[26–32] In these studies, %*G* depended on many reaction parameters, including the monomer concentration, initiator type and concentration, reaction temperature and time, and pretreatment or modification of Cell. For instance, Gupta and Khandekar[29] grafted NIPAM polymer onto Cell with a ceric amonium nitrate–nitric acid iniator system, and they found a maximum N content of 5.06%. In this study, quite high %*G* and G_E values was

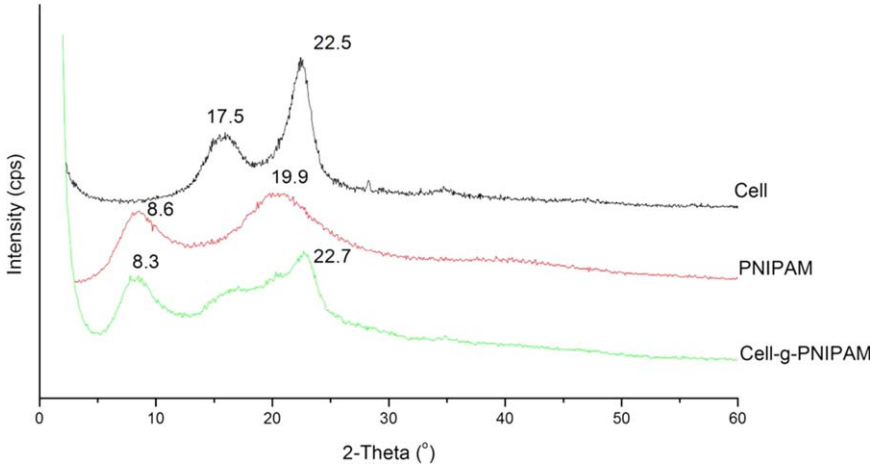

Figure 2. XRD patterns of Cell, PNIPAM, and their graft copolymer (Cell-*g*-PNIPAM). [Color figure can be viewed in the online issue, which is available at wileyonlinelibrary.com.]

obtained compared to those given in the literature. In our study, the initiator was added in four equal portions to the reaction mixture. In preliminary experiments, the gradual addition of initiator increased %*G* by about twice. In graft copolymerization, %*G* increased with increasing initiator amount, but with high amounts of CAN, the precipitation of active radical species was probably a result of the fast termination reactions onto the Cell surface. Thus, the diffusion of monomer toward the active Cell surface was prevented, and homopolymerization reactions dominated grafting.[26,29] In the case of the gradual addition of initiator, we supposed that the oxidative termination reactions of Ce^{4+} ions due to a higher concentration of radicals were prevented, and active centers on the Cell were used efficiently for grafting. Thus, new active radicals were created on the Cell backbone in a controlled manner, and this enhanced %*G*.

Swelling and Thermoresponsive Properties

The swelling isotherm of the Cell-*g*-PNIPAM copolymer at 10°C and the deswelling isotherms at various temperatures are given in Figure 5. We observed that *S*% reached 96% of the equilibrium value at 10 h at 10°C. *S*% decreased with increasing temperature. Furthermore, the equilibrium time decreased with increasing temperature. The S % values of the Cell-*g*-PNIPAM polymer at various temperatures are given in Table I. Also, the water release (%) values at these temperatures were calculated according to the following equation, and the values are given in the same table:

$$\text{Water release}\,(\%) = \left[\left(S_{e,10^\circ\text{C}} - S_{e,T}\right)\right] / S_{e,10^\circ\text{C}} \qquad (5)$$

where $S_{e,10^\circ\text{C}}$ and $S_{e,T}$ are the equilibrium swelling degrees at 10°C and at a given temperature, respectively.

It is shown in Table I that the S % decreased with increasing temperature, and the amount of water released increased. A 97.5% release of water by swollen graft copolymer at 50°C is a very high release performance for a polymer that contains thermosensitivity only in its graft chains.

Thermosensitive polymers change their physical properties drastically and induce phase transition in response to temperature changes.[33,34] They swell below their LCSTs and shrink above their LCSTs. PNIPAM has sharp phase-transition properties; it forms well-hydrated expanded random-coil structures below its LCST and forms hydrophobic structures by rapid dehydration

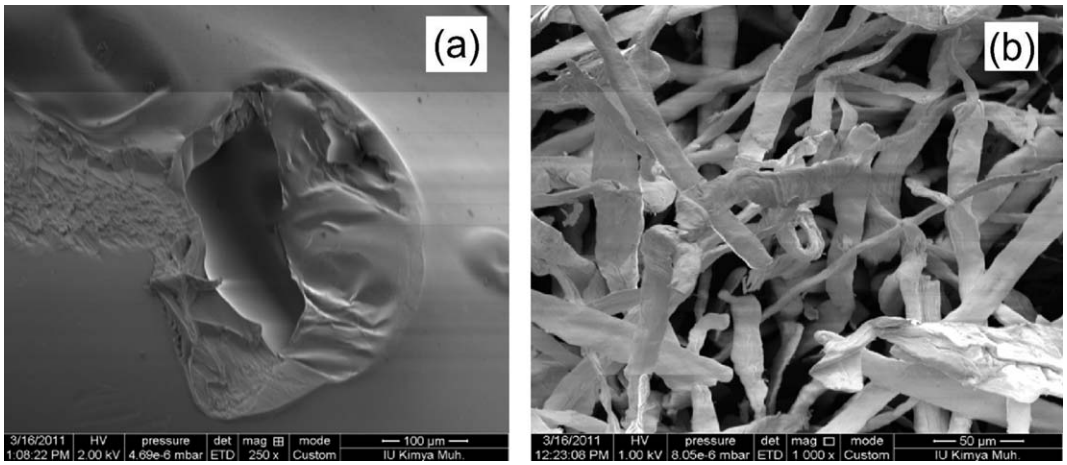

Figure 3. SEM images of (a) PNIPAM and (b) Cell.

Applied Polymer SCIENCE

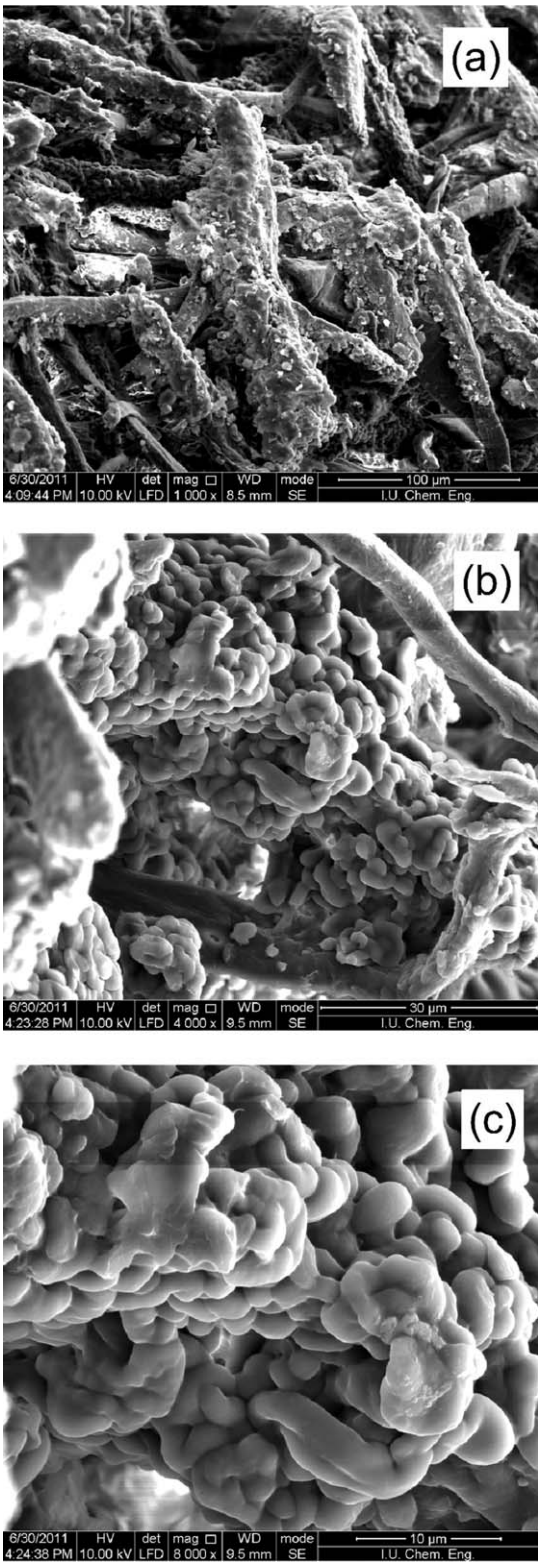

Figure 4. SEM images of the graft copolymer with different magnitudes.

above LCST.[34] The Cell-*g*-PNIPAM copolymer also swelled at low temperatures and shrunk at high temperatures.

To determine the thermosensitivity of the polymer, the DSC technique was used. The DSC curves of Cell and Cell-*g*-PNIPAM are shown in Figure 6. A sharp phase transition was observed for the graft copolymer at 32.4°C, but Cell did not exhibit a volume phase transition under the same conditions. In literature, it is stated that linear PNIPAM exhibited a sharp, fast, and discontinuous phase transition at 32–34°C.[34–36] It is interesting that the LCST of the graft

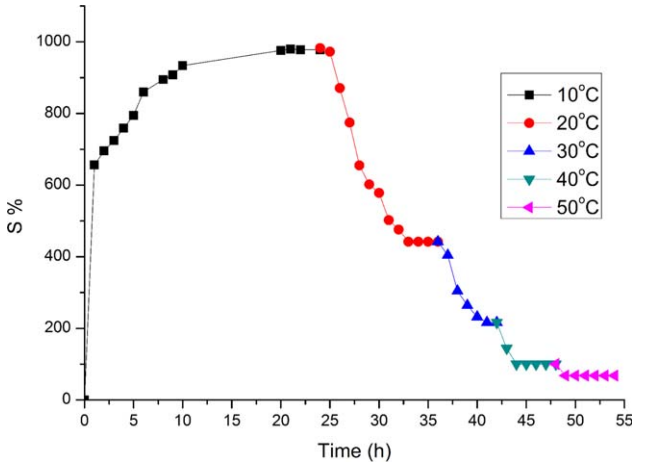

Figure 5. Swelling and deswelling isotherms of the graft copolymer at 10°C and various other temperatures. [Color figure can be viewed in the online issue, which is available at wileyonlinelibrary.com.]

Table I. *S*% and Water Release Values of Cell-*g*-PNIPAM at Various Temperatures

Temperature (°C)	*S*%[a]	Water release (%)
10	983	0
20	468	52.4
30	313	68.2
40	73	92.6
50	25	97.5

[a] *S*% was determined at equilibrium.

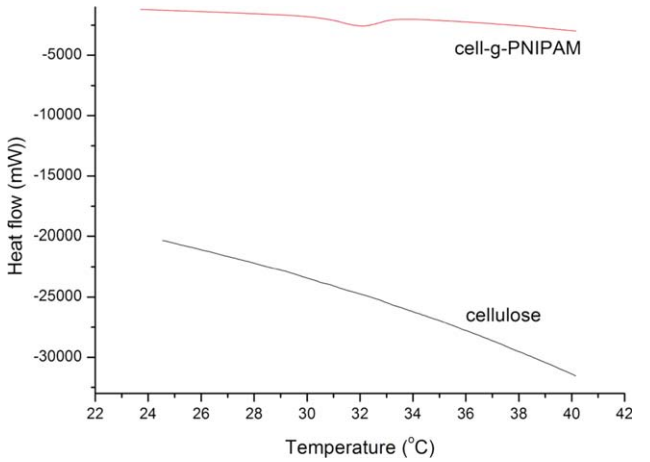

Figure 6. DSC diagram of Cell and the graft copolymer (Cell-*g*-PNIPAM). [Color figure can be viewed in the online issue, which is available at wileyonlinelibrary.com.]

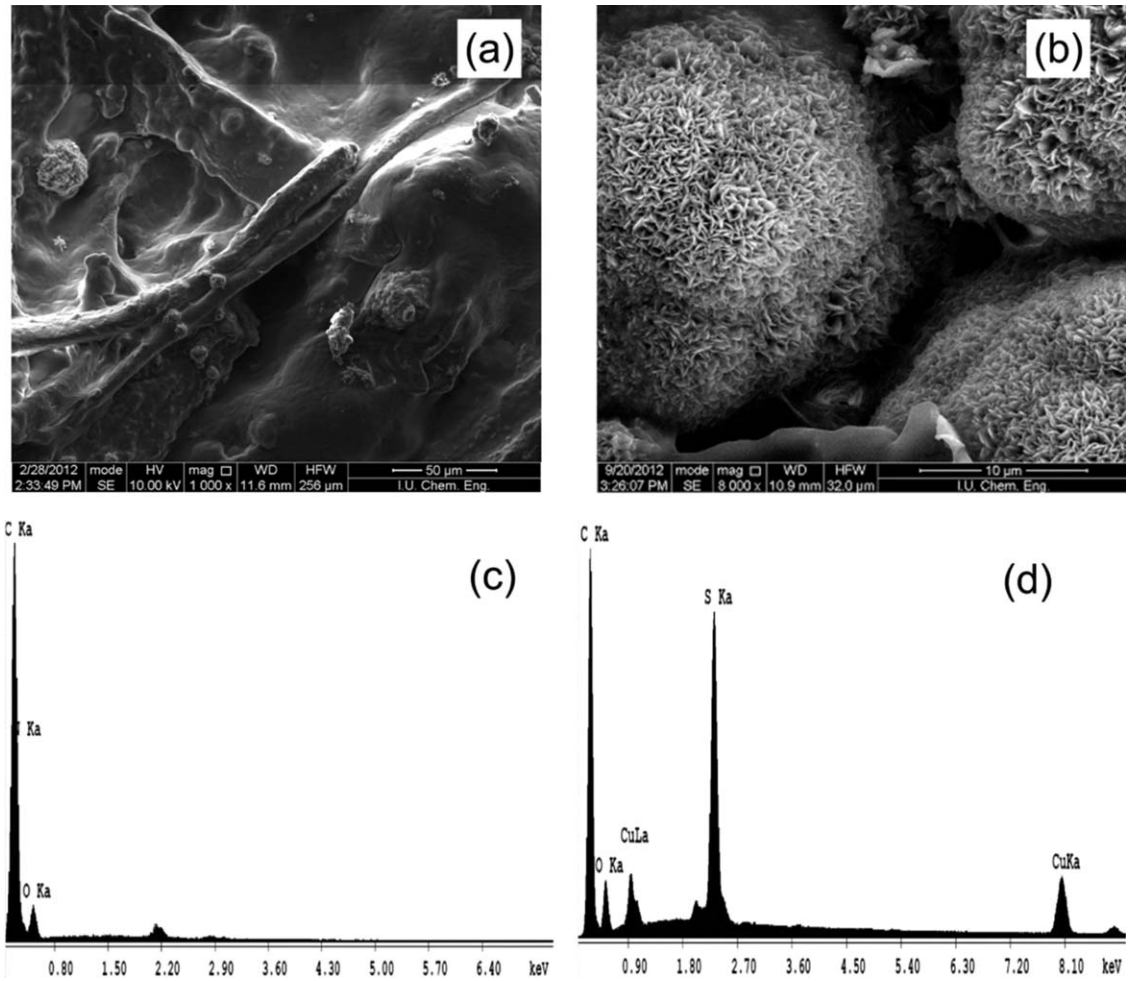

Figure 7. (a,b) SEM images of the graft copolymer after adsorption and EDS spectra of the graft copolymer (c) before and (d) after adsorption.

copolymer was close to the value of the PNIPAM homopolymer. The graft copolymer showed a thermosensitivity similar to that of PNIPAM. This situation supposed that the Cell-*g*-PNIPAM had freely mobile long graft chains in the structure. It is stated in the literature that during deswelling in thermosensitive polymers, the rapid dehydration of graft chains strongly aggregated with hydrophobic intermolecular forces and that the attractive forces operating between dehydrated chains were larger in a polymer having longer graft chains.[37] The sharp phase-transition properties of Cell-*g*-PNIPAM were the result of the stepwise addition of the CAN initiator in the polymerization. Thus, the product obtained without gradual addition did not show a sharp phase transition in the preliminary experiments (its DSC curve was not given).

Adsorption Studies

The SEM–EDS patterns of the graft copolymer after the adsorption process are given in Figure 7. A shown in these SEM images, there were obvious morphological differences between the graft copolymer and Cu–SDBS-adsorbed copolymer [Figures 4(a) and 7(a,b)]. As shown in Figure 7(a), in the presence of the Cu–SDBS complexes, the surface of the polymer was covered by a thin layer and became smooth. However, in some areas, the formation of agglomerates was observed. The SEM pattern of these agglomerates is shown with higher magnification in Figure 7(b). In the EDS spectrum of these agglomerates [Figure 7(d)], the appearances of the Cu and S peaks confirmed the adsorption of the Cu–SDBS complex on the polymer surface. The Cell-*g*-PNIPAM copolymer was not efficient in the removal of Cu(II) ions without SDBS. In adsorption experiments, Q of the polymer was found as 2.4×10^{-2} mmoL/g.

Figure 8 shows the effect of the initial Cu(II)-ion concentration on Q. Q of the Cell-*g*-PNIPAM copolymer increased with increasing initial Cu(II)-ion concentration. The adsorption process corresponded to a sigmoidal (S)-type adsorption isotherms in the Giles classification system.[38] In the S curves in the Giles classifications system, the initial direction of curvature shows that the adsorption occurs more easily as the concentration rises. Isotherms of S class occur by two reasons. First, solute–solute attractive forces at the surface may cause cooperative adsorption, which leads to the S shape.[39] Second,

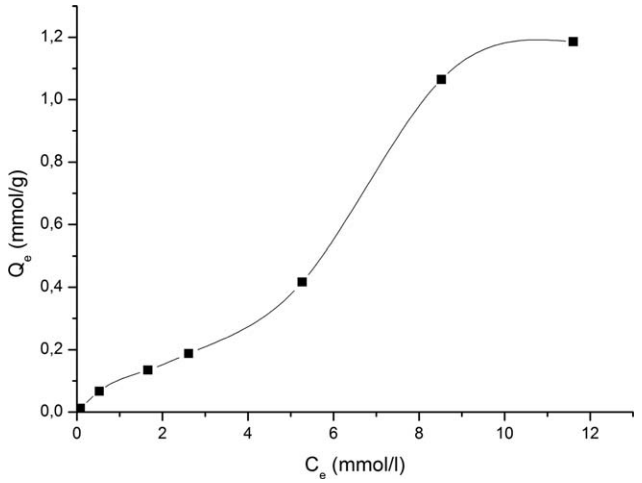

Figure 8. Cu(II)-ion adsorption isotherm of the graft copolymer at 50°C.

the sorption of a solute may be inhibited by a competing reaction within the solution, such a complexation reaction with a ligand.[40]

This type of isotherm is always the result of at least two opposite mechanisms. For instance, nonpolar organic compounds are a typical case. In the initial step of adsorption, the surface of the sorbent is covered by these compounds, and other organic molecules in the medium are also adsorbed easily on the surface. This phenomenon is called *cooperative adsorption*.[41] In our system, after the inflection point, Q increased rapidly. We supposed that the coverage of the polymer surface by the hydrophobic surfactant–metalion complex caused the increases in the hydrophobic interactions and Q values of the copolymer. As it is known, the SDBS could complex with Cu(II) ions by the aid of hydrophilic $-SO_3$ groups, and 1 mol of Cu(II) ions reacts with 2 mol of SDBS, so a hydrophobic Cu-SDBS complex ($Cu(SDBS)_2$) formed. In the adsorption process above the LCST value, hydrophobic interactions between the hydrophobic alkyl tail group and aromatic benzene ring of the $Cu(SDBS)_2$ complex and methyl group of the PNIPAM units occurred. When the surfactant–metalion complex concentration increased, lateral surfactant–surfactant interactions came into play. Once the critical association value was reached (before the inflection point), the adsorbed amount of complex increased sharply toward its saturation value. In the literature, this phenomenon was also observed for the adsorption of the surfactants.[42–45]

Figure 9 shows the effect of the treatment time on the adsorption of Cu(II) ions by the Cell-*g*-PNIPAM copolymer at 50°C. Q increased with the treatment time and reached adsorption equilibrium to a large extent in 10 h. Q_e was found to be 1.18 mmoL/g polymer. In the literature, many studies have been reported on the adsorption of metal ions by thermosensitive polymers.[14–19,46,47] In some of these studies, the PNIPAM copolymers obtained with various monomers having functional groups that could be complexed with metal ions have been used, and their use has been investigated in the removal of Cu(II) ions from aqueous solutions.[14,18,46,47] In the studies that were similar to our study, a homopolymer of PNIPAM or hydrogel was used in the removal of metal ions in the presence of complexing substances,[13,16,17,19] and the Cu(II)-ion removal capacity changed between 0.03 and 0.3 mmol/g. Q of the Cell-*g*-PNIPAM copolymer was very high in comparison to the values published in similar works.

To express the mechanism of the adsorption of metal ions onto Cell-*g*-PNIPAM, the kinetic data were analyzed by pseudo-first-order and pseudo-second-order equations. The differential equation of the pseudo-first-order kinetic model is as follows:

$$\frac{dQ_e}{dt} = k_1(Q_e - Q_t) \tag{6}$$

where Q_e and Q_t refer to the amount of metal ion adsorbed (mmoL/g) at equilibrium and at time t (h), respectively, and k_1 is the rate constant of pseudo-first-order adsorption (h^{-1}). The integration of eq. (6) for the boundary conditions (from $t = 0$ and $Q_t = 0$ to t and Q_t) gives the following equation:

$$\log\left(\frac{Q_e}{Q_e - Q_t}\right) = \frac{k_1}{2.303}t \tag{7}$$

This is the integrated rate law for a pseudo-first-order reaction. Equation (7) can be linearized to the following form:

$$\log(Q_e - Q_t) = \frac{\log(Q_e - k_1)}{2.303}t \tag{8}$$

where k_1 and the theoretical maximum metalion adsorption capacity (Q_e) can be determined from the slope of the plot of $\log(Q_e - Q_t)$ against t and the intercept.

On the other hand, the differential form of a pseudo-second-order equation is expressed as follows:

$$\frac{dQ_t}{dt} = k_2(Q_e - Q_t)^2 \tag{9}$$

where k_2 is the rate constant of pseudo-second-order adsorption (g $mmol^{-1}$ h^{-1}). The integration of eq. (9) for the boundary conditions gives

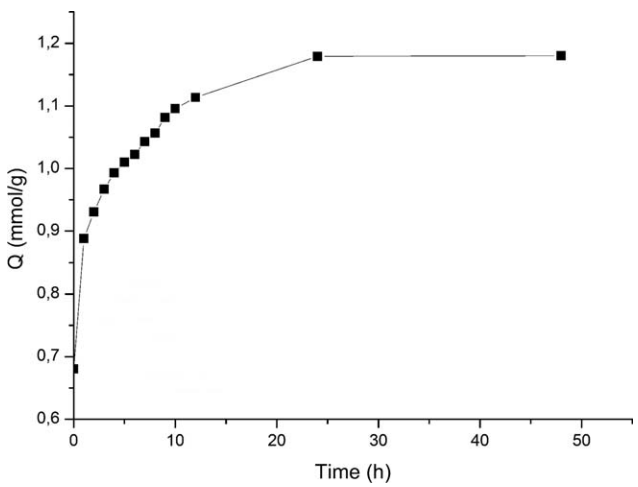

Figure 9. Effect of the treatment time on the Q of the graft copolymer.

Table II. k_1 and k_2 Values for the $Cu(SDBS)_2$ Complex on the Grafted Copolymer

Pseudo-first-order kinetic model			Pseudo-second-order kinetic model			
Q_e (mmol/g)	k_1 (h^{-1})	r_1^2	Q_e (mmol/g)	k_2 (g $mmol^{-1}$ h^{-1})	r_i (mmol g^{-1} h^{-1})	r_2^2
0.611	0.2489	0.9188	1.196	1.1419	1.633	0.9994

$$\frac{1}{(Q_e - Q_t)} = \frac{1}{Q_e} + k_2 t \quad (10)$$

which is the integrated rate law for a pseudo-second-order reaction. Equation (10) can be linearized to the following form:

$$\frac{t}{Q_t} = \frac{1}{k_2 Q_e^2} + \left(\frac{1}{Q_e}\right) t \quad (11)$$

The values of k_2, Q_e, and the initial adsorption rate ($r_i = k_2 Q_e^2$, mmol g^{-1} h^{-1}) can be obtained from the slope and intercept of the plot of t/Q_t against t.

The validity of these two models can be checked by analysis of the linearized plots. The rate constants, calculated Q_e values, and correlation coefficients are given in Table II. We determined that the pseudo-second-order kinetic model fit the data obtained better than the first-order model for the adsorption of the Cu–SDBS complex onto Cell-*g*-PNIPAM as the correlation coefficient (r_2^2) was closer to 1 ($r_2^2 > 0.999$) than that of the first-order kinetics (r_1^2). Moreover, the Q_e value for the second-order kinetics was close to the Q_e value obtained experimentally (experimental $Q_e = 1.18$ mmol/g). All of these pointed to the fact that second-order kinetics best explained the overall observed rate, and this means that the adsorption of the $Cu(SDBS)_2$ complex may have been dependent on the amount of complex on the surface of the polymer and the amount of complex sorbed at equilibrium. The rate of adsorption was proportional to the square of the number of unoccupied sites.

Figure 10 shows the effect of the initial pH on Q of the Cell-*g*-PNIPAM copolymer. We observed that Q increased with increasing pH in the experimental region. In low pH values, because the increase in the hydrogen ion concentration could prevent the formation of the Cu–SDBS complex, Q decreased.[13] Also, the reusability of the Cell-*g*-PNIPAM copolymer was investigated in adsorption–desorption cycles carried out at 50−10°C (Figure 11). We observed that the copolymer could be used repeatedly without a loss of capacity.

CONCLUSIONS

A thermoresponsive Cell-*g*-PNIPAM copolymer with a high %*G* was obtained by the grafting of a NIPAM monomer onto Cell. FTIR, XRD, and SEM analyses showed that the PNIPAM chain was grafted onto the Cell fiber successfully, and %*G* was found to be 69.5% from the elemental analysis results. A sharp phase transition was observed at 32.4°C and was similar to that of PNIPAM in the DSC curve of the graft copolymer. The deswelling experiments revealed that the graft copolymer released 97.5% of its water at 50°C.

The Cell-*g*-PNIPAM copolymer was used in the removal of Cu(II) ions from aqueous solution in the presence of SDBS. Q reached equilibrium in approximately 10 h, and a quite high Q (1.18 mmol/g) was observed. The capacity increased with the increase in the initial pH of the solutions in the experimental region. We found from the kinetic studies that the adsorption kinetics of the graft copolymer followed a pseudo-second-order model. S-type adsorption in the Giles classification system was observed. The adsorption experiments showed that these thermoresponsive Cell-*g*-PNIPAM copolymers with high Q values could be used effectively for the adsorption of the Cu–SDBS complex as novel adsorbent materials for the removal of heavy-metal ions.

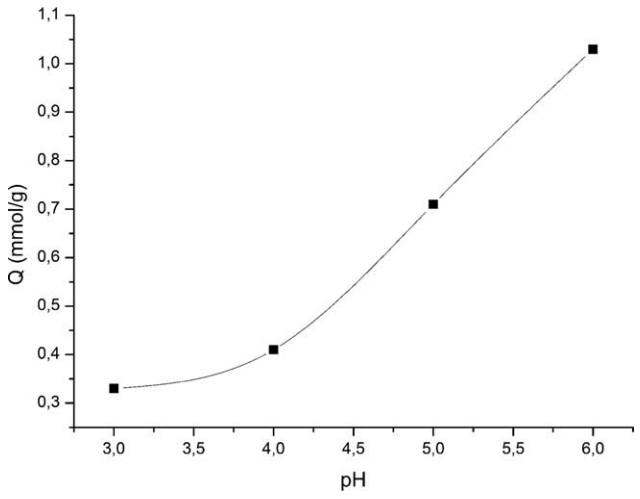

Figure 10. Effect of pH on the Q of the graft copolymer.

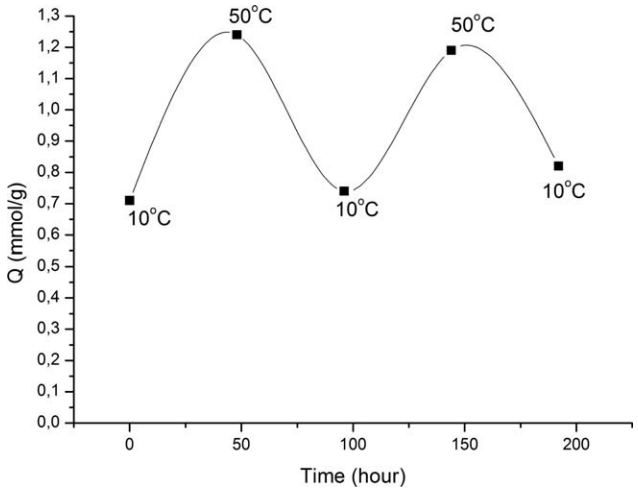

Figure 11. Changes in Q of the graft copolymer during the adsorption and desorption cycles.

ACKNOWLEDGMENTS

This work was supported by The Scientific and Technical Research Council of Turkey (TUBITAK) (contract grant number MAG/110M153). The authors thank Ali Durmus and Gamze Çetin for their help with the DSC analysis.

REFERENCES

1. Nriagu, J. O.; Pacyna, J. M. *Nature* **1988**, *333*, 134.
2. Mance, G. Pollution Threat of Heavy Metals in Aquatic Environments; Elsevier Science: New York, **1987**.
3. Dean, J. G.; Bosqui, F. L.; Lanouette, K. H. *Environ. Sci. Technol.* **1979**, *6*, 416.
4. Patterson, J. W. Industrial Wastewater Treatment Technology; Butterworth: Boston, **1985**.
5. Ahluwalia, S. S.; Goyal, D. *Bioresour. Technol.* **2007**, *98*, 2243.
6. Nurchi, V. M.; Villaescusa, I. *Coord. Chem. Rev.* **2008**, *252*, 1178.
7. Brown, P. A.; Gill, S. A.; Allen, S. *J. Water Res.* **2000**, *34*, 3907.
8. Jin, L.; Bai, R. B. *Langmuir* **2002**, *18*, 9765.
9. Denizli, A.; Sanli, N.; Garipcan, B.; Patir, S.; Alsancak, G. *Ind. Eng. Chem. Res.* **2004**, *43*, 6095.
10. Duran, A.; Soylak, M.; Tuncel, S. A. *J. Hazard. Mater.* **2008**, *155*, 114.
11. Kasgoz, H.; Durmus, A.; Kasgoz, A. *Polym. Adv. Technol.* **2008**, *19*, 213.
12. Kasgoz, H. *Polym. Bull.* **2006**, *56*, 517.
13. Tokuyama, H.; Iwama, T. *Langmuir* **2007**, *23*, 13104.
14. Yamashita, K.; Nishimura, T.; Nango, M. *Polym. Adv. Technol.* **2003**, *14*, 189.
15. Ju, X. J.; Zhang, S. B.; Zhou, M. Y.; Xie, R.; Yang, L.; Chu, L. Y. *J. Hazard. Mater.* **2009**, *167*, 114.
16. Tokuyama, H.; Hiseada, J.; Nii, S.; Sakohara, S. *Sep. Purif. Technol.* **2010**, *71*, 83.
17. Tokuyama, H.; Iwama, T. *Sep. Purif. Technol.* **2009**, *68*, 417.
18. Tokuyama, H.; Yanagawa, K.; Sakohara, S. *Sep. Purif. Technol.* **2006**, *50*, 8.
19. Tokuyama, H.; Kanehara, A. *React. Funct. Polym.* **2007**, *67*, 136.
20. Singha, A. S.; Shama, A.; Thakur, V. K. *Int. J. Polym. Anal. Charact.* **2008**, *13*, 447.
21. Ozbas, Z.; Esen, E.; Gurdag, G.; Kasgoz, H. Proceeding of the 25th National Chemistry Congress with International Participation, Erzurum, Turkey, June 26–July 2, **2011**.
22. Oh, S. Y.; Yoo, D. I.; Shin, Y.; Seo, G. *Carbohydr Res.* **2005**, *340*, 417.
23. Liu, C. F.; Zhang, A. P.; Li, W. Y.; Sun, R. C. In Ionic Liquids: Applications and Perspectives; Kokorin, A., Ed.; InTech: New York, **2011**, Chapter 5, pp. 81.
24. Emik, S.; Gurdag, G. *J. Appl. Polym. Sci.* **2006**, *100*, 428.
25. Ekici, S. *J. Mater. Sci.* **2011**, *46*, 2843.
26. Carrillo, F.; Defays, B.; Colom, X. *Eur. Polym. J.* **2008**, *44*, 4020.
27. Kubota, H.; Shiobara, N. *React. Funct. Polym.* **1998**, *37*, 219.
28. Ifuku, S.; Kadla, J. F. *Biomacromolecules* **2008**, *9*, 3308.
29. Gupta, K. C.; Khandekar, K. *Biomacromolecules* **2003**, *4*, 758.
30. Yang, H. R.; Esteves, A. C. C.; Zhu, H. J.; Wang, D. J.; Xin, J. H. *Polymer* **2012**, *53*, 3577.
31. Kim, Y. S.; Kadla, J. F. *Biomacromolecules* **2010**, *11*, 981.
32. Lu, J.; Li, J.; Yi, M.; Ha, H. F. *Radiat. Phys. Chem.* **2001**, *60*, 625.
33. Zhang, X. Z.; Zhuo, R. X. *Eur. Polym. J.* **2000**, *36*, 2301.
34. Otake, K.; Inomata, H.; Konno, M.; Saito, S. *Macromolecules* **1990**, *23*, 283.
35. Han, Y. A.; Choi, J. H.; Park, D. J.; Ji, B. C. *Polym. Test.* **2002**, *21*, 913.
36. Tokuhiro, T.; Amiya, T.; Mamada, A.; Tanaka, T. *Macromolecules* **1991**, *24*, 2936.
37. Kaneko, Y.; Sakai, K.; Kikuchi, A.; Yoshida, R.; Sakurai, Y.; Okano, T. *Macromolecules* **1995**, *28*, 7717.
38. Giles, C. H.; Mac Even, T. H.; Nakhwa, S. H.; Smith, D. *J. Chem. Soc.* **1960**, *3*, 3973.
39. Giles, C. H.; Smith, D.; Huitson, A. *J. Colloid Interface Sci.* **1974**, *106*, 226.
40. Hinz, C. *Geoderma* **2001**, *99*, 225.
41. Limousin, G.; Gaudet, J.-P.; Charlet, L.; Szenknect, S.; Barthes, V.; Krimissa, M. *Appl. Geochem.* **2007**, *22*, 249.
42. Groisman, L.; Rav-Acha, C.; Gerstl, Z.; Mingelgrin, U. *Appl. Clay Sci.* **2004**, *24*, 159.
43. Smith, J. A.; Galan, A. *Environ. Sci. Technol.* **1995**, *29*, 685.
44. Rea, R. L.; Parks, G. A. In Chemical Modelling of Aqueous Systems II; Melchior, D. C., Bassett, R. L., Eds.; ACS Symposium Series 416; American Chemical Society: Washington, DC, **1990**; p 260.
45. Geffroy, C.; Cohen Stuart, M. A.; Wong, K.; Cabane, B.; Bergeron, V. *Langmuir* **2000**, *16*, 6422.
46. Kanazawa, R.; Yoshida, T.; Gotoh, T.; Sakohara, S. *J. Chem. Eng. Jpn.* **2004**, *37*, 59.
47. Ozkahraman, B.; Acar, I.; Emik, S. *Clean Soil Air Water* **2011**, *39*, 658.